Partially Nondestructive Continuous Detection of Individual Traveling Optical Photons

Mahdi Hosseini, Kristin M. Beck, Yiheng Duan, Wenlan Chen, and Vladan Vuletić*
Department of Physics and Research Laboratory of Electronics, Massachusetts Institute of Technology, Cambridge, Massachusetts 02139, USA
(Received 26 August 2015; published 19 January 2016)

We report the continuous and partially nondestructive measurement of optical photons. For a weak light pulse traveling through a slow-light optical medium (signal), the associated atomic-excitation component is detected by another light beam (probe) with the aid of an optical cavity. We observe strong correlations of $g_{sp}^{(2)} = 4.4(5)$ between the transmitted signal and probe photons. The observed (intrinsic) conditional nondestructive quantum efficiency ranges between 13% and 1% (65% and 5%) for a signal transmission range of 2% to 35%, at a typical time resolution of 2.5 μs. The maximal observed (intrinsic) device nondestructive quantum efficiency, defined as the product of the conditional nondestructive quantum efficiency and the signal transmission, is 0.5% (2.4%). The normalized cross-correlation function violates the Cauchy-Schwarz inequality, confirming the nonclassical character of the correlations.

DOI: 10.1103/PhysRevLett.116.033602

Photons are unique carriers of quantum information that can be strongly interfaced with atoms for quantum state generation and processing [1–9]. Quantum state detection, a particular type of processing, is at the heart of quantum mechanics and has profound implications for quantum information technologies. Photons are standardly detected by converting a photon's energy into a measurable signal, thereby destroying the photon. Nondestructive photon detection, which is of interest for many quantum optical technologies [10–12], is possible through strong nonlinear interactions [12] that ideally form a quantum nondemolition measurement [13]. To date, quantum nondemolition measurement of single microwave photons bound to cooled cavities has been demonstrated with high fidelity using Rydberg atoms [14–16], and in a circuit cavity quantum electrodynamics system using a superconducting qubit [17].

For quantum communication and many other photonics quantum information applications [18,19], it is desirable to detect traveling optical photons instead of photons bound to cavities. Previously, a single-photon transistor was realized using an atomic ensemble inside a high finesse cavity where one stored photon blocked the transmission of more than one cavity photon and could still be retrieved [5]. Such strong cross-modulation [20] can be used for all-optical destructive detection of the stored optical photon, but the parameters in that experiment did not allow nondestructive detection with any appreciable efficiency. High-efficiency pulsed nondestructive optical detection has recently been achieved using a single atom in a cavity [21]. In that implementation, the atomic state is prepared in 250 μs, altered by the interaction with an optical pulse reflected from the cavity, and read out in 25 μs.

In this Letter, we realize partially nondestructive, continuous detection of traveling optical photons with microsecond time resolution. The signal photons to be detected propagate through an atomic ensemble as slow-light polaritons [22] under conditions of electromagnetically induced transparency (EIT) [23]. The signal polariton's atomic-excitation component is nondestructively detected via the polarization change on another light field (probe), enhanced by an optical cavity. We observe positive correlations between the signal and probe photons of $g_{sp}^{(2)} = 4.4(5)$, and use the measured correlation function to calculate the conditional nondestructive quantum efficiency Q. We achieve efficiencies Q between 13% and 1% at a signal transmission T_s between 2% and 35%, with a maximum device nondestructive quantum efficiency $Q \times T_s$ of 0.47% at a maximum signal input rate of 300 kHz.

The nondestructive measurement scheme and atomic level structure are shown in Fig. 1. A laser-cooled atomic ensemble of ^{133}Cs atoms is held in a cigar-shaped dipole trap that partly overlaps with the fundamental mode of the optical cavity. A signal light resonant with the $|g\rangle \rightarrow |c\rangle$ transition propagates orthogonal to the cavity axis through the ensemble. A control laser induces an EIT transmission window that slows down the signal light to a typical group velocity of 300 m/s and reversibly maps it onto a collective atomic excitation in state $|d\rangle$ [22]. This atomic population couples strongly to the σ^+ polarized light which is simultaneously resonant with the optical cavity and the $|d\rangle \rightarrow |e\rangle$ transition, blocking its transmission through the cavity [20,24,25]. To generate a useful positive detection signal in transmission, we add σ^- reference light and probe the cavity continuously with horizontally polarized light. The reference light interacts only weakly with the atoms: the atomic coupling strength on the $|d\rangle \rightarrow |f\rangle$ transition is 45 times smaller than the strength of the σ^+ transition and is also detuned from resonance by $\Delta/2\pi = 6$ MHz by the 5.2 G magnetic field along the cavity axis (z). Light transmitted through the cavity is then analyzed in a

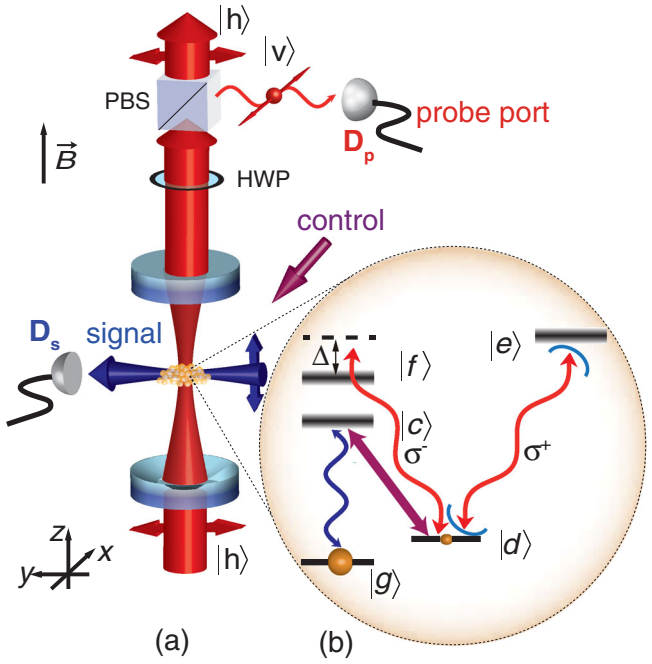

FIG. 1. (a),(b) The π-polarized signal light travels with slow group velocity through the atoms by means of EIT on the $|g\rangle \leftrightarrow |c\rangle \leftrightarrow |d\rangle$ transitions. The associated atomic-excitation component is nondestructively detected via cavity light in the geometric overlap between the atomic ensemble and the cavity mode. Input cavity light is linearly polarized such that, in the absence of signal photons, the probe port of the polarization beam splitter (PBS) ideally remains dark. Whenever a signal photon traverses the atomic medium in the cavity, the transmission of the σ^+ polarized light through the cavity is blocked. The atomic levels are $|g\rangle = |6S_{1/2}; F = 3, m_F = 3\rangle$, $|c\rangle = |6P_{3/2}; 3, 3\rangle$, $|d\rangle = |6S_{1/2}; 4, 4\rangle$, $|e\rangle = |6P_{3/2}; 5, 5\rangle$, and $|f\rangle = |6P_{3/2}; 5, 3\rangle$, where F, m_F are the hyperfine quantum numbers.

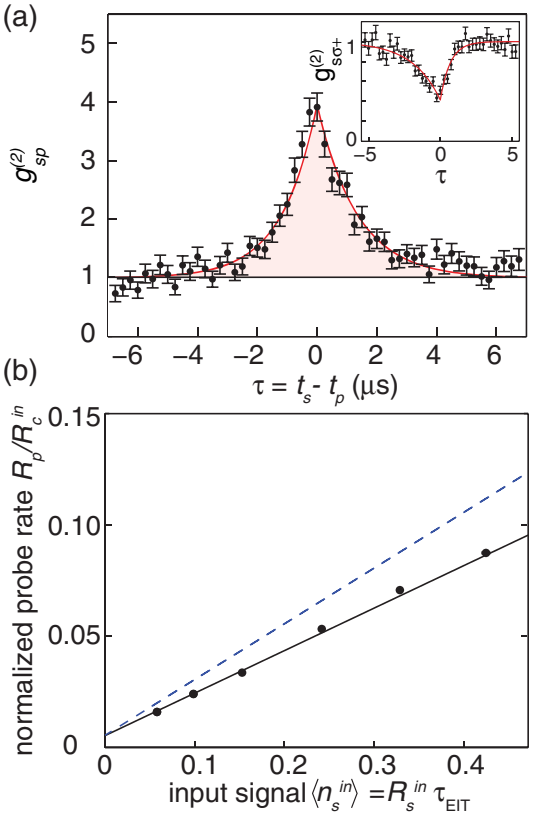

FIG. 2. (a) Signal-probe correlation function $g^{(2)}_{sp}$ is plotted as a function of separation time τ between signal (t_s) and probe (t_p) photons. The decay time constant for negative (positive) times $\tau_< = 1.2(2)$ μs [$\tau_> = 1.3(2)$ μs] is consistent with the cavity decay time (EIT lifetime) [20]. This measurement is done with mean input cavity photon number $\langle n_c^{\rm in}\rangle = R_c^{s=0}\tau_c/q_c = 3.7$, cavity path detection efficiency $q_c = 0.2$, $\tau_c = (\kappa/2)^{-1} = 2$ μs, and Rabi frequency $\Omega/2\pi = 1.9$ MHz. The inset shows the cross-correlation function for signal and σ^+-polarized cavity photons, measured for $\langle n_c^{\rm in}\rangle = 0.1$ and $\Omega/2\pi = 2.6$ MHz. The observed signal-probe anticorrelation is $g^{(2)}_{s\sigma^+}(0) = 0.41(7)$. In this and all following figures, statistical error bars are plotted when they are larger than the points and indicate one standard deviation. (b) Normalized detected probe rate $R_p/R_c^{s=0}$, plotted against input signal photon number $\langle n_s^{\rm in}\rangle = R_s^{\rm in}\tau_{\rm EIT}/q_s$. The slope of the solid fitted line is 0.20(1). The dashed line represents the maximum possible probe rate with a slope of $\varepsilon_{id} = 0.25$. For this measurement, $\langle n_c^{\rm in}\rangle = 1.2$, $q_s = 0.3$, and $\Omega/2\pi = 1.3$ MHz, giving $\tau_{\rm EIT} = 1.4$ μs.

horizontal or vertical basis. Vertically polarized light (probe port) corresponds to detection, as the probe port is dark in the absence of signal photons.

Quantum correlations between detected outgoing signal and probe photons are the signature of nondestructive detection. The cross-correlation function $g^{(2)}_{sp} = \langle n_s n_p\rangle / \langle n_s\rangle\langle n_p\rangle$ can be understood as the likelihood of measuring the signal twice: first measuring it nondestructively with our cavity QED system, which results in a detected probe photon ($n_p = 1$), and then checking the first measurement by measuring the signal photon again destructively ($n_s = 1$). The cross-correlation function in Fig. 2(a) with zero-time value $g^{(2)}_{sp}(0) = 4.0(3)$ demonstrates that simultaneous nondestructive and destructive measurements of the signal photon occur four times more often than randomly. This value also agrees well with the directly observed blocking of σ^+-polarized cavity photons by a signal photon [inset to Fig. 2(a)], and with the theoretical expectations for our system's cooperativity $\eta = 4.3$ and relevant optical depth $\mathcal{D} \simeq 3$ (see the Supplemental Material [26]). The increased $\mathcal{D}$ accounts for the improvement over previously published results with the same apparatus [20].

To confirm the linearity of the system, we plot the probe rate normalized to the empty cavity output rate, $R_p/R_c^{s=0}$, against the average input signal photon number per EIT lifetime $\langle n_s^{\rm in}\rangle = R_s^{\rm in}\tau_{\rm EIT}/q_s$ in Fig. 2(b). Here, $R_s^{\rm in}/q_s$ is the measured input rate corrected for the finite detection efficiency $q_s = 0.3$. Under ideal circumstances, an incident cavity photon emerges in the probe port with

the probability $\varepsilon_{id} = 1/4$ in the presence of a signal photon, indicated in the figure as a dashed line. Achieving this limit requires a strong single-atom-cavity coupling (cooperativity $\eta \gg 1$) [27], large ensemble optical depth inside the cavity region $\mathcal{D} \gg 1$, and sufficiently slowly traveling signal photons $\tau_{\mathrm{EIT}}/\tau_c > 1$, where τ_c is the cavity lifetime. Even with finite cooperativity η and optical depth, we measure $\varepsilon = 0.20(1)$. This number is the detection probability per input cavity photon and includes both nondestructive and destructive detection of the signal photon. The nonzero offset in Fig. 2(b) at $\langle n_s^{\mathrm{in}} \rangle = 1$ corresponds to the background noise in the average measurement. The observed linear increase in probe rate for $\langle n_s^{\mathrm{in}} \rangle < 1$ also confirms the sensitivity of our experiment at the single photon level. However, unlike output correlations, this average signal neither distinguishes between destructive and nondestructive detection events nor does it reveal the time resolution of the detector. Destructive detection events correspond to decohered polaritons, i.e., atomic population in state $|d\rangle$, and hence have the same effect on the cavity light as traveling signal photons.

To study only those events when we preserve the signal photon, we define the conditional nondestructive quantum efficiency Q to be the conditional probability for a correlated photon to be detected in the probe port when a signal photon is present: $Q = \langle n_s n_p \rangle / \langle n_s \rangle - \langle n_p \rangle$ for $\langle n_s \rangle \ll 1$. (Note that the second term $\langle n_p \rangle = \langle n_p \rangle \langle n_s \rangle / \langle n_s \rangle$ is necessary to remove uncorrelated (random) coincidences between signal and probe photons.) The time scale for this conditioning is defined by the typical correlation time: this conditional nondestructive quantum efficiency Q is precisely the area under $g^{(2)}(\tau) - 1$ [the shaded area in Fig. 2(a)] multiplied by the average rate of detected photons at the probe port, R_p: $Q = R_p \int [g^{(2)}(\tau) - 1] d\tau$. Q evaluates to 10% for the cross-correlation function plotted in Fig. 2(a). The time resolution is the sum of the positive- and negative-correlation times, $\tau_> + \tau_< = 2.5(4)\ \mu$s [20]. Since Q scales with the detected rate at the probe port, finite probe photon detection efficiency q_p directly reduces Q. The total detection efficiency for probe photons $q_p = 0.2$ is the product of detector efficiency (0.45), fiber coupling and filter losses (0.7), and cavity outcoupling losses (0.66). Correcting for these linear losses gives the intrinsic conditional nondestructive quantum efficiency $Q/q_p = 50\%$. Single photon detectors with better than 0.99 efficiency exist at our wavelength, so only improving the optics and detectors outside of our vacuum chamber would already allow us to achieve a Q of 30%. We define the device nondestructive quantum efficiency as the probability for an input photon to be nondestructively detected. It is equal to $Q \times T_s$, the product of the conditional nondestructive quantum efficiency and the signal transmission. Figure 3 explores the tradeoff between these two factors. Q scales linearly with the input cavity photon number [Fig. 3(a)], as with increasing cavity input rate it becomes more likely for a randomly arriving cavity photon to "hit" a signal photon and perform the detection. At the same time, the signal transmission T_s degrades exponentially with the input cavity rate due to cavity-induced decoherence of the signal polariton, as seen in Fig. 3(b). Slower signal polaritons (smaller control Rabi frequency Ω) are more likely to be "hit" by a cavity photon, and thus have a larger nondestructive quantum efficiency but also have a lower transmission due to a greater decoherence for a given cavity photon number. The choice of Rabi frequency changes the detector speed but does not improve the tradeoff between efficiency and transmission; the inset of Fig. 3(b) shows that observed quantum efficiency as a function of signal transmission collapses to a single curve for all measured Rabi frequencies.

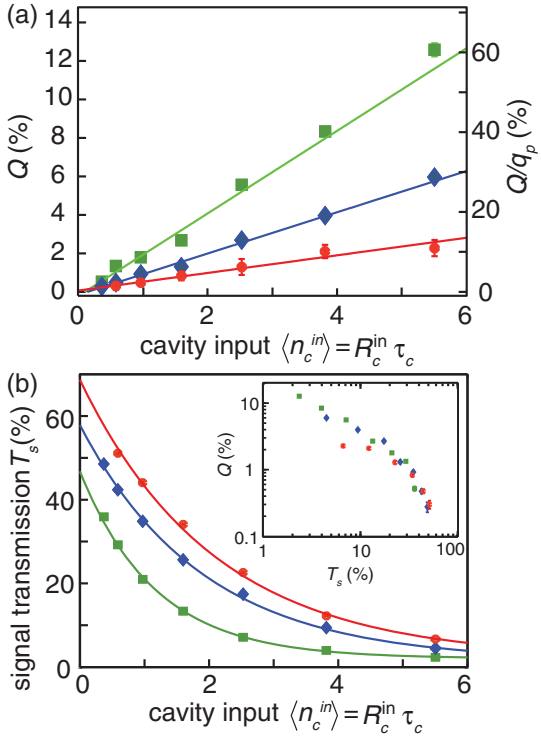

FIG. 3. (a) The observed conditional nondestructive quantum efficiency Q is plotted against mean cavity photon number $\langle n_c^{\mathrm{in}} \rangle$ with mean $R_s^{\mathrm{in}} = 2.8 \times 10^5\ \mathrm{s}^{-1}$. The slope of the fitted curves (solid lines) is $dQ/d\langle n_c^{\mathrm{in}} \rangle = \{10(2), 5(1), 1.9(5)\}\%$ for $\Omega/2\pi = \{1.8, 2.9, 3.5\}$ MHz (top to bottom) and represents the observed detection efficiency per input cavity photon. (b) Signal transmission T_s for the same data presented in (a). Exponential fits give $1/e$ transmission at cavity photon numbers of $\{1.2(1), 1.9(1), 2.1(1)\}$ for $\Omega/2\pi = \{1.8, 2.9, 3.5\}$ MHz (bottom to top), respectively. The inset displays the nondestructive quantum efficiency Q as a function of signal transmission for the same Rabi frequencies as in (a) and (b).

Figure 4 plots the device nondestructive quantum efficiency and the error probability P_{err} as a function of input photon number. The maximal observed (intrinsic) device nondestructive quantum efficiency is 0.47% (2.4%). P_{err} is

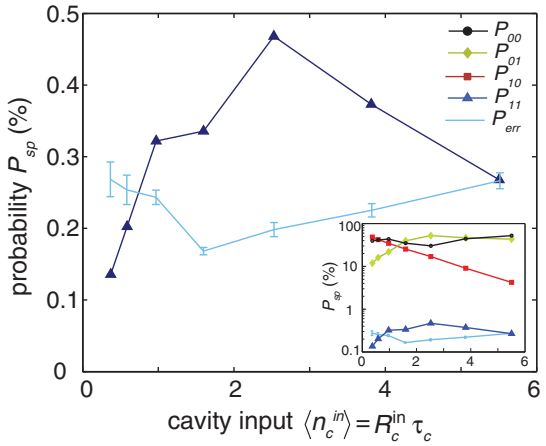

FIG. 4. Device nondestructive quantum efficiency ($P_{11} = Q \times T_s$) and error probability P_{err} for joint detection of signal and probe outputs for $\Omega/2\pi = 2.9$ MHz. P_{11} is calculated assuming one input signal photon. P_{err} represents the false detection of probe photons in the absence of signal photons. The inset displays all four characterizing probabilities P_{sp} with s, $p = \{0, 1\}$ (see text) and P_{err} under the same conditions.

the probability of having a false detection event when no signal photon is present. Considering these together, the detector achieves a nondestructive signal-to-noise ratio of 2.4. We further characterize the performance for single input photons by calculating by the four probabilities P_{sp} to detect the $s = \{0, 1\}$ signal and $p = \{0, 1\}$ probe photons given one input signal photon. These probabilities can be obtained from measured quantities in the limit $\langle n_s^{\mathrm{in}}\rangle \ll 1$ using the relations $P_{11}/(P_{11} + P_{10}) = Q$, $P_{11} + P_{10} = T_s$, $P_{01} + P_{11} = \langle n_p\rangle/\langle n_s^{\mathrm{in}}\rangle$, and $\sum P_{sp} = 1$. These probabilities describe different aspects of the nondestructive detection. In particular, the device nondestructive quantum efficiency is P_{11} and the state preparation probability $P_{11}/(P_{11} + P_{01}) \simeq 4\%$ represents the probability of having an outgoing signal photon if a photon is present at the probe port.

In our system, the transmission of detected signal photons is limited to about 70% by the standing wave nature of our cavity probe, which imprints a grating onto the detected polariton and reduces its readout efficiency in the original mode. In addition, since the atomic medium extends outside the cavity mode, the detection localizes the signal polariton in a finite region of the ensemble, and the corresponding spectral broadening outside the EIT transmission window reduces the signal transmission by 30% (see the Supplemental Material [26]). Finally, cavity photon scattering into free space, which destroys the signal polariton, occurs with a finite probability $2\eta/(1 + \eta)^2 = 0.3$. The combination of these effects explains the observed transmission reduction for the signal.

To further enhance the effective optical density of the medium, we also carried out an experiment where the signal propagates twice through the medium (see the Supplemental Material [26]). In this case, we observed slightly stronger correlations of $g_{sp}^{(2)}(\tau = 0) = 4.4(5)$ due to the larger effective optical depth. To remove classical correlations from the observed cross-correlation, we normalize the cross-correlation function to the autocorrelations measured at the signal and probe ports of $g_{ss}^{(2)} = 1.6(3)$ and $g_{pp}^{(2)} = 5.6(1)$. The resulting normalized quantum correlation $G_{sp} = (g_{sp}^{(2)})^2/(g_{ss}^{(2)} g_{pp}^{(2)}) = 2.7(8)$ at $\tau = 0$ violates the Cauchy-Schwarz inequality [28], $G < 1$, and confirms that our interactions are nonclassical.

The key to the nondestructive photon measurement scheme demonstrated here is the strong interaction between one atom and a cavity photon [29–31] (large single-atom cooperativity $\eta \gg 1$), in combination with the strong collective interaction of atoms with signal photons (large optical depth $\mathcal{D} \gg 1$ inside the cavity). Both quantities can be further improved in our experiment. For realistic values $\mathcal{D} = 10$ and $\eta = 20$, we expect a device nondestructive quantum efficiency exceeding 55% with a conditional nondestructive quantum efficiency of about 80% and a signal transmission of about 70%. An interaction of this kind enables many quantum applications such as the projection of a coherent state of a light pulse into a photon number state [16], the implementation of nearly deterministic photonic quantum gates through nondestructive measurement and conditional phase shift [11], engineering exotic quantum states of light [32] or nondeterministic noiseless amplification for entanglement distillation [33].

The authors would like to thank Arno Rauschenbeutel for insightful discussions. This work was supported by the NSF and the Air Force Office of Scientific Research. K. M. B. acknowledges support from the NSF IGERT under Grant No. 0801525.

*Corresponding author.
vuletic@mit.edu

[1] Y. O. Dudin and A. Kuzmich, Strongly interacting Rydberg excitations of a cold atomic gas, Science **336**, 887 (2012).
[2] T. Peyronel, O. Firstenberg, Q.-Y. Liang, S. Hofferberth, A. V. Gorshkov, T. Pohl, M. D. Lukin, and V. Vuletić, Quantum nonlinear optics with single photons enabled by strongly interacting atoms, Nature (London) **488**, 57 (2012).
[3] C. Lang, D. Bozyigit, C. Eichler, L. Steffen, J. M. Fink, A. A. Abdumalikov, Jr., M. Baur, S. Filipp, M. P. da Silva, A. Blais, and A. Wallraff, Observation of Resonant Photon Blockade at Microwave Frequencies Using Correlation Function Measurements, Phys. Rev. Lett. **106**, 243601 (2011).
[4] I. Fushman, D. Englund, A. Faraon, N. Stoltz, P. Petroff, and J. Vučković, Controlled phase shifts with a single quantum dot, Science **320**, 769 (2008).
[5] W. Chen, K. M. Beck, R. Bücker, M. Gullans, M. D. Lukin, H. Tanji-Suzuki, and V. Vuletić, All-optical switch and

transistor gated by one stored photon, Science **341**, 768 (2013).
[6] H. Gorniaczyk, C. Tresp, J. Schmidt, H. Fedder, and S. Hofferberth, Single-Photon Transistor Mediated by Interstate Rydberg Interactions, Phys. Rev. Lett. **113**, 053601 (2014).
[7] D. Tiarks, S. Baur, K. Schneider, S. Dürr, and G. Rempe, Single-Photon Transistor Using a Förster Resonance, Phys. Rev. Lett. **113**, 053602 (2014).
[8] P. Michler, A. Kiraz, C. Becher, W. V. Schoenfeld, P. M. Petroff, L. Zhang, E. Hu, and A. Imamoglu, A quantum dot single-photon turnstile device, Science **290**, 2282 (2000).
[9] H. Tanji, S. Ghosh, J. Simon, B. Bloom, and V. Vuletić, Heralded Single-Magnon Quantum Memory for Photon Polarization States, Phys. Rev. Lett. **103**, 043601 (2009).
[10] J. Sperling, W. Vogel, and G. S. Agarwal, Quantum state engineering by click counting, Phys. Rev. A **89**, 043829 (2014).
[11] K. Nemoto and W. J. Munro, Nearly Deterministic Linear Optical Controlled-NOT Gate, Phys. Rev. Lett. **93**, 250502 (2004).
[12] N. Imoto, H. A. Haus, and Y. Yamamoto, Quantum nondemolition measurement of the photon number via the optical Kerr effect, Phys. Rev. A **32**, 2287 (1985).
[13] P. Grangier, J. A. Levenson, and J.-P. Poizat, Quantum nondemolition measurements in optics, Nature (London) **396**, 537 (1998).
[14] G. Nogues, A. Rauschenbeutel, S. Osnaghi, M. Brune, J. M. Raimond, and S. Haroche, Seeing a single photon without destroying it, Nature (London) **400**, 239 (1999).
[15] S. Gleyzes, S. Kuhr, C. Guerlin, J. Bernu, S. Deléglise, U. B. Hoff, M. Brune, J.-M. Raimond, and S. Haroche, Quantum jumps of light recording the birth and death of a photon in a cavity, Nature (London) **446**, 297 (2007).
[16] C. Guerlin, J. Bernu, S. Deléglise, C. Sayrin, S. Gleyzes, S. Kuhr, M. Brune, J.-M. Raimond, and S. Haroche, Progressive field-state collapse and quantum non-demolition photon counting, Nature (London) **448**, 889 (2007).
[17] B. R. Johnson, M. D. Reed, A. A. Houck, D. I. Schuster, L. S. Bishop, E. Ginossar, J. M. Gambetta, L. DiCarlo, L. Frunzio, S. M. Girvin, and R. J. Schoelkopf, Quantum nondemolition detection of single microwave photons in a circuit, Nat. Phys. **6**, 663 (2010).
[18] E. Knill, R. Laflamme, and G. J. Milburn, A scheme for efficient quantum computation with linear optics, Nature (London) **409**, 46 (2001).
[19] N. Gisin and R. Thew, Quantum communication, Nat. Photonics **1**, 165 (2007).
[20] K. M. Beck, W. Chen, Q. Lin, M. Gullans, M. D. Lukin, and V. Vuletić, Cross Modulation of Two Laser Beams at the Individual-Photon Level, Phys. Rev. Lett. **113**, 113603 (2014).
[21] A. Reiserer, S. Ritter, and G. Rempe, Nondestructive detection of an optical photon, Science **342**, 1349 (2013).
[22] M. Fleischhauer and M. D. Lukin, Dark-State Polaritons in Electromagnetically Induced Transparency, Phys. Rev. Lett. **84**, 5094 (2000).
[23] S. E. Harris, Electromagnetically induced transparency, Phys. Today **50**, No. 7, 36 (1997).
[24] A. Imamoğlu, H. Schmidt, G. Woods, and M. Deutsch, Strongly Interacting Photons in a Nonlinear Cavity, Phys. Rev. Lett. **79**, 1467 (1997).
[25] M. Soljačić, E. Lidorikis, J. Joannopoulos, and L. Hau, Ultralow-power all-optical switching, Appl. Phys. Lett. **86**, 171101 (2005).
[26] See Supplemental Material at http://link.aps.org/supplemental/10.1103/PhysRevLett.116.033602 for detailed experimental method, calculation of detection and transmission probabilities, derivation of quantum efficiency and QND requirements.
[27] H. Tanji-Suzuki, I. D. Leroux, M. H. Schleier-Smith, M. Cetina, A. Grier, J. Simon, and V. Vuletić, Interaction between atomic ensembles and optical resonators: Classical description, Adv. At. Mol. Opt. Phys. **60**, 201 (2011).
[28] J. F. Clauser, Experimental distinction between the quantum and classical field-theoretic predictions for the photoelectric effect, Phys. Rev. D **9**, 853 (1974).
[29] J. McKeever, A. Boca, A. D. Boozer, J. R. Buck, and H. J. Kimble, Experimental realization of a one-atom laser in the regime of strong coupling, Nature (London) **425**, 268 (2003).
[30] J. Volz, R. Gehr, G. Dubois, J. Estève, and J. Reichel, Measurement of the internal state of a single atom without energy exchange, Nature (London) **475**, 210 (2011).
[31] I. Shomroni, S. Rosenblum, Y. Lovsky, O. Bechler, G. Guendelman, and B. Dayan, All-optical routing of single photons by a one-atom switch controlled by a single photon, Science **345**, 903 (2014).
[32] B. Wang and L.-M. Duan, Engineering superpositions of coherent states in coherent optical pulses through cavity-assisted interaction, Phys. Rev. A **72**, 022320 (2005).
[33] S. L. Zhang, S. Yang, X. B. Zou, B. S. Shi, and G. C. Guo, Protecting single-photon entangled state from photon loss with noiseless linear amplification, Phys. Rev. A **86**, 034302 (2012).